

THE CORRECT LOCAL DESCRIPTION FOR TRACKING IN RINGS

ÉTIENNE FOREST

¹ *Center for Beam Physics, Lawrence Berkeley Laboratory,
Berkeley, CA, USA 94720*

MICHAEL F. REUSCH, DAVID L. BRUHWILER

² *Grumman Corporate Research Center*

and ALI AMIRY

³ *Physics Department, University of California, Los Angeles*

(Received 7 October 1993; in final form 10 February 1994)

We discuss the absolute minimum knowledge required to design a symplectic integrator for rings. We include details about: (1) symplectic integrators for compound bends, (2) coordinate patches for bends with arbitrary entry and exit angles, (3) general fringe field effects, (4) arbitrary magnet displacements, and (5) radiation effects in electron rings. Of course, we expect the usual automatic differentiation to be implemented in such integrators and to be linked with a perturbation theory package capable of analyzing symplectic and non-symplectic maps for the beam envelope analysis (calculation of equilibrium second-order moments).

KEY WORDS: Particle dynamics, storage rings, synchrotron radiation

1 INTRODUCTION

The computation of transfer maps in small machines, whether by tracking or Taylor series, requires special attention to the details and geometry of individual magnets. Through the years, it has been customary to use simplified models for the simulation of circular rings. In these models, ideal quadrupoles and ideal bends are linear in the transverse variables. Fringe fields are totally absent except for vertical focusing in bends. These approximations can break down as rings get smaller and their focusing gets stronger. The purpose of this paper is to convince the reader that it is possible to write an explicit symplectic integrator for the ideal ring in terms of local Hamiltonians and local coordinate frames. In the process, we hope that the reader will realize that ideal rings are not “linear”.^a This realization had been

^a The statements apply to circular rings. In other fields of beam transport, such as spectrometer designs and electron microscopy, the nonlinear contribution of the ideal element is often a limiting factor and therefore is always included in simulations.

implemented partially in a code called “TEAPOT” by Schachinger and Talman.¹ In this code, they correctly included the “square root” effect, making the body of ideal quadrupoles and sector bends nonlinear. “TEAPOT” remains a second-order integrator that does not account for fringe fields or radiation, which makes it inappropriate for small machines. In addition, the actual tracking loop of TEAPOT was written in terms of a global coordinate frame, a practice we strongly discourage. To our knowledge the first usage of a symplectic integrator for the design of an actual small machine can be found in Reference 2. Finally, we would like to point out that the need to include “square-root” effects or some quadrupole fringe field is not confined to small rings (see Reference 3). In the end, the only way to find out if the traditional approximations are valid is to compare tracking results from an approximate code (large ring) with those of a small-machine code.

1.1 *Local versus global*

This paper is rooted in a fundamental aspect of circular ring dynamics that demands a deeper appreciation of the dichotomy between local and global concepts. The local concepts are the physical quantities necessary to propagate a particle or a distribution of particles for an infinitesimal distance ds . For single-particle dynamics, these concepts simply amount to the Lorentz force. The global concepts are quantities computed for the sake of our human understanding. They are the results of our feeble attempt to understand the process of continuously circulating a beam inside a machine. These include, for example, “beta functions,” tunes shifts, resonance strengths, etc. We believe^b that this dichotomy must be preserved in a proper theoretical description of circular dynamics; therefore, the tracking of a particle with an integrator must involve only local concepts. The Hamiltonian must be dictated locally by the symmetries of the magnets. It is mathematically ill-advised to integrate a particle using a frame of reference dictated by perturbation theory on the full ring, a practice not too uncommon in the field e.g., integration through wigglers.⁴ The “lattice functions,” the “closed orbit,” the “dispersions,” and all other global concepts have no part to play in the construction of a tracking code.

On the other hand, the analysis of the motion, which is not described here, is done on the one-turn map. The local Hamiltonian is totally irrelevant to this enterprise: this is why we have been advocating for years a Hamiltonian-free perturbation theory.

In summary, the production of the one-turn map, gotten from tracking data or Taylor-series approximation and its subsequent analysis (computation of lattice functions, equilibrium emittances, etc., which is accomplished by rewriting the one-turn map in terms of Lie operators) must be totally decoupled, computationally as well as conceptually. We invite the reader to become acquainted with this point of view by reading Reference 5. It is absolutely fundamental to a proper understanding of this paper.

^b “We believe” is a euphemism and a compromise between the authors. Some of us would prefer, “It is our unshakable belief”!

1.2 *Lego Block*^c

It is not always possible to find a global frame of reference for the exact Hamiltonian of the ring which describes the entire machine in simple terms. In fact, if one reads in Reference 5, it is argued that is not desirable to look for a global frame. Remember that theorists have always liked a simple global Hamiltonian because of their analysis techniques (Hamiltonian perturbation theory). We reject perturbation theory based on the Hamiltonian, and therefore this ceases to be a good reason. Instead, one selects for each magnet, and even for sections of a magnet, a preferential local coordinate system or “patch.” The local frames are entirely driven by the local shape and symmetries of the field (i.e., the magnet). These patches are then joined smoothly by certain coordinate transformations. In fact, we must ensure that the various elements of the ring are joined smoothly like the Lego blocks used by children around the world. In Reference 5 we define the most fundamental block of all: the bend block. The bend is an element whose purpose (usually but not necessarily) is to bend the orbit by approximately an angle θ . The bend is made of two faces, each having a frame of reference attached to it. The y axes (vertical) of the frames are parallel, and the x axes (horizontal) meet at exactly an angle θ . An arc of circle of length L passes through the origin of both frames at a 90° angle. Of course, the straight element is a special case of the bend. (L stays constant but θ goes to zero.)

In Reference 5 it is argued that all elements are bends from the point of view of the reference frames and can be glued to each other using an $x - y$ rotation when the ring is, for example non-planar. Torsion^d is never needed in circular ring physics if one applies the block decomposition of the lattice and abandons the hopeless and useless construction of a global Hamiltonian.

In this paper the reader will notice that we always insist on maintaining the Lego structure of the element. To do this, we introduce various coordinate transformations. This is particularly important in the misalignment section. We urge the reader again to read Reference 5.

1.3 *Content*

To be more precise we will show how coordinate transformations are used to design an integrator for bends of cylindrical and Cartesian geometry. In particular, we will discuss how one can write a symplectic integrator for small machines. It is assumed that the code is linked to some automatic differentiation package for map computation and analysis.^{6,7} We do not discuss this topic here, but it is essential for effective and accurate usage of a simulation package.

In Section 2, we introduce the exact solution of the constant-**B**-field sector bend. We indicate how to construct an integrator in the presence of a vector potential term in the sector bend (combined-function bend).

^c Lego is a registered trade mark of Interlego A.G. Is is a marvelous block set with which children of all ages should play.

^d More precisely, torsion is needed at most at one location in the ring.

In Section 3, we introduce the canonical transformation $Y_{\text{rot}}^F(\theta)$, which is the map for a “wedge.” It is an essential ingredient for the construction of the arbitrary bend and for the proper Lego treatment of misalignments. This map is gotten from the sector bend map by a limiting process.

In Section 4, we introduce the exact solution of the constant-**B**-field parallel-face bend and its associated integrator in the presence of a multipole component. Again, a limiting process is used on the results of the sector bend.

In Section 5, we use the results of the previous sections to describe bends with arbitrary geometry.

In Section 6, we discuss the issue of fringe fields and how to compute them as exact zero-length insertions, which by definition preserve the Lego-block structure. This can be done by automatic differentiation techniques,⁸ implicit symplectic integration, or direct ordinary integration.

In Section 7, we give a flavor of the misalignment of a complex element. This is done with Y_{rot} , X_{rot} , $x - y$ (transverse) rotations, drifts and translations. These transformations were used by Healy in his thesis;⁹ however he did not make use of the Lego blocks explicitly, which is unfortunate. Historically, the first use of Y_{rot} can be found in Dragt’s paper on chromaticities in small rings.¹⁰

In Section 8, we give an introduction to the treatment of radiation and the computation of the beam envelope following the treatment of Hirata and Ruggiero.¹¹ Appendix A discusses approximate fringe maps that account for mainly vertical focussing. In Appendix B, we make the connection with the approximate treatment of Chao.¹² The Sands formalism can also be derived as a limiting case of the envelope formalism, as shown in Reference 13.

2 THE COMBINED FUNCTION SECTOR BEND

We start with a Hamiltonian in cylindrical coordinates for the body of the sector bend:

$$\begin{aligned}
 H &= H_1 + H_2 \\
 H_1 &= - \left(1 + \frac{x}{\rho_c} \right) \sqrt{(1 + \delta)^2 - p_x^2 - p_y^2} + b_0 x + b_0 \frac{x^2}{2\rho_c} \\
 H_2 &= V(x, y, \rho_c) \\
 \mathbf{w} &= (x, p_x, y, p_y, \delta, \tau); \delta \text{ is conjugate to the path length}^e \tau \\
 \rho_c &= \text{curvature of the frame of reference} \\
 p_x, p_y &\text{ and } \delta \text{ are normalized by } p_0 \\
 b_0 &= \frac{q B_y}{p_0} = \text{normalized field strength} .
 \end{aligned} \tag{2.1}$$

^e Here we assume ultrarelativistic particles; hence path length and time of flight are the same. This constraint can be relaxed if necessary.

In the treatment of non-ideal rings, it is very important to distinguish the radius of curvature in the actual \mathbf{B} -field ($\rho = \frac{1}{b_0}$) from ρ_c , which is the curvature of the cylindrical frame of reference or to be more general, the radius of the arc of circle on which our Lego-bend block is sitting. This allows us to treat the most general type of magnet. In fact, the curve described by $x = 0$ need not be an actual trajectory. It needs to be only in the neighborhood of the actual closed orbit. Therefore it is a mistake to think that complex frames of references with torsion are needed whenever the fields are non-ideal. Such frames are needed only if the beam-pipe itself is strongly helical. This is never the case even in a helical wiggler.⁴

Going back to Equation (2.1), we notice that the Ruth algorithm¹⁴⁻¹⁷ is applicable in its extended sense whenever H is split into two^f exactly solvable parts as it is in Equation (2.1). The Hamiltonian H_2 is solvable and it leads to the usual kick. Notice that we explicitly included the dependence of ρ_c which is present when one solves for the multipole components in a cylindrical frame. It also turns out that H_1 is exactly solvable. This has been exploited by others as well.¹⁸ The solution is:

$$\begin{aligned}
 x^f &= \frac{\rho_c}{b_0} \left(\frac{1}{\rho_c} \sqrt{(1+\delta)^2 - p_x^{f2} - p_y^2} - \frac{dp_x^f}{ds} - b_0 \right) \\
 p_x^f &= p_x \cos\left(\frac{s}{\rho_c}\right) + \left(\sqrt{(1+\delta)^2 - p_x^2 - p_y^2} - b_0(\rho_c + x) \right) \sin\left(\frac{s}{\rho_c}\right) \\
 y^f &= y + \frac{p_y s}{b_0 \rho_c} + \frac{p_y}{b_0} \left\{ \arcsin\left(\frac{p_x}{\sqrt{(1+\delta)^2 - p_y^2}}\right) - \arcsin\left(\frac{p_x^f}{\sqrt{(1+\delta)^2 - p_y^2}}\right) \right\} \\
 p_y^f &= p_y \\
 \delta^f &= \delta \\
 \tau^f &= \tau + \frac{(1+\delta)s}{b_0 \rho_c} + \frac{(1+\delta)}{b_0} \left\{ \arcsin\left(\frac{p_x}{\sqrt{(1+\delta)^2 - p_y^2}}\right) \right. \\
 &\quad \left. - \arcsin\left(\frac{p_x^f}{\sqrt{(1+\delta)^2 - p_y^2}}\right) \right\}
 \end{aligned} \tag{2.2}$$

^f Thanks to Suzuki and Yoshida, the real answer is two or more solvable parts.¹⁷

In Equation (2.2), we distinguish the curvature of the frame of reference ρ_c from the actual magnetic field b_0 . Let us denote the map of (2.2) as $S(s, \rho_c, b_0)$. The map for the potential $V(x, y, \rho_c)$ which we denote by $K(s, \rho_c)$ is just:

$$p_x^f = p_x - s \frac{\partial V}{\partial x} \quad p_y^f = p_y - s \frac{\partial V}{\partial y} \quad (2.3)$$

According to the theory of explicit symplectic integration, the full map for the body of the sector bend can be written as:⁸

$$M_{\angle}(\theta) = \exp(-s : H_1 + H_2 :) \approx \prod_{i=1}^{N_k} S(s_{1;i}, \rho_c, \rho_c) K(s_{2;i}, \rho_c) + O(s^{k+1}), \quad (2.4)$$

where k is the order of the integrator.

A final note: in Equation (2.4), the perfect sector bend map is evaluated at $b_0 = \frac{1}{\rho_c}$. This ensures that, for the ideal bend, the arc of the circle of angle $\theta = \frac{s}{\rho_c}$ is an actual trajectory, namely $\mathbf{w} = (0, 0, 0, 0, 0, 0)$, goes into $\mathbf{w} = (0, 0, 0, 0, 0, s)$. In the absence of a potential V , the map S matches the Lego block of Reference 5. Of course, any fluctuation of the vertical \mathbf{B} -field must be handled by the potential V .

3 THE TRANSFORMATION $Y_{\text{ROT}}^F(\theta)$

In Figure 1, we display schematically the boundary between two media. For reasons having to do with the internal symmetries of each medium, we have decided to change the orientation of the coordinate systems at the point of entry ‘‘O’’. Readers should convince themselves that this rotation of the coordinate system represents a propagation through medium 1 in cylindrical coordinates, which have been expressed around the point ‘‘O’’.

We can analytically derive expressions for this rotation in the ideal bend medium by taking appropriate limits:

$$Y_{\text{rot}}^F(\theta) = \lim_{\substack{\rho_c \rightarrow 0; s \rightarrow 0 \\ \frac{s}{\rho_c} = \theta}} S(s, \rho_c, b_0). \quad (3.1)$$

⁸ Here we adopt Dragt’s notation for the Lie operator. The operator $:f:$ acting on a function g is defined as the Poisson bracket $[f, g]$. All maps such as $S(s, \rho_c, b_0)$ or $\exp(:f:)$ are functional maps. See appendix B, Equation (B3), for a definition of the map in terms of its associated coordinate transformation. See also Reference 13.

The result of Equation (3.1) are:

$$\begin{aligned}
 x^f &= x \cos(\theta) + \frac{\left\{ x p_x \sin(2\theta) + \sin^2(\theta) \left(2x \sqrt{(1+\delta)^2 - p_x^2 - p_y^2} - b_0 x^2 \right) \right\}}{\sqrt{(1+\delta)^2 - p_x^2 - p_y^2} + \sqrt{(1+\delta)^2 - p_x^2 - p_y^2} \cos(\theta) - p_x \sin(\theta)} \\
 p_x^f &= p_x \cos(\theta) + \sin(\theta) \left\{ \sqrt{(1+\delta)^2 - p_x^2 - p_y^2} - b_0 x \right\} \\
 y^f &= y + \frac{\theta p_y}{b_0} + \frac{p_y}{b_0} \left\{ \arcsin \left(\frac{p_x}{\sqrt{(1+\delta)^2 - p_y^2}} \right) - \arcsin \left(\frac{p_x^f}{\sqrt{(1+\delta)^2 - p_y^2}} \right) \right\} \\
 \tau^f &= \tau + \frac{\theta(1+\delta)}{b_0} + \frac{(1+\delta)}{b_0} \left\{ \arcsin \left(\frac{p_x}{\sqrt{(1+\delta)^2 - p_y^2}} \right) \right. \\
 &\quad \left. - \arcsin \left(\frac{p_x^f}{\sqrt{(1+\delta)^2 - p_y^2}} \right) \right\}. \tag{3.2}
 \end{aligned}$$

The expression in Equation (3.2) is valid for any value of b_0 , however, it is made out of diverging expressions at $b_0 = 0$. Hence, it is useful to derive the field-free formula also. We denote this map by $Y_{\text{rot}}(\theta)$, it is a drift in ‘‘cylindrical’’ coordinates:

$$\begin{aligned}
 x^f &= \frac{x}{\cos(\theta) \left(1 - \frac{p_x \tan(\theta)}{\sqrt{(1+\delta)^2 - p_x^2 - p_y^2}} \right)} \\
 p_x^f &= p_x \cos(\theta) + \sin(\theta) \sqrt{(1+\delta)^2 - p_x^2 - p_y^2} \\
 y^f &= y + \frac{p_y x \tan(\theta)}{\sqrt{(1+\delta)^2 - p_x^2 - p_y^2} \left(1 - \frac{p_x \tan(\theta)}{\sqrt{(1+\delta)^2 - p_x^2 - p_y^2}} \right)} \\
 \tau^f &= \tau + \frac{(1+\delta)x \tan(\theta)}{\sqrt{(1+\delta)^2 - p_x^2 - p_y^2} \left(1 - \frac{p_x \tan(\theta)}{\sqrt{(1+\delta)^2 - p_x^2 - p_y^2}} \right)}. \tag{3.3}
 \end{aligned}$$

The map $Y_{\text{rot}}(\theta)$ is the map ‘‘PROT’’ pioneered by Dragt in Reference 10.

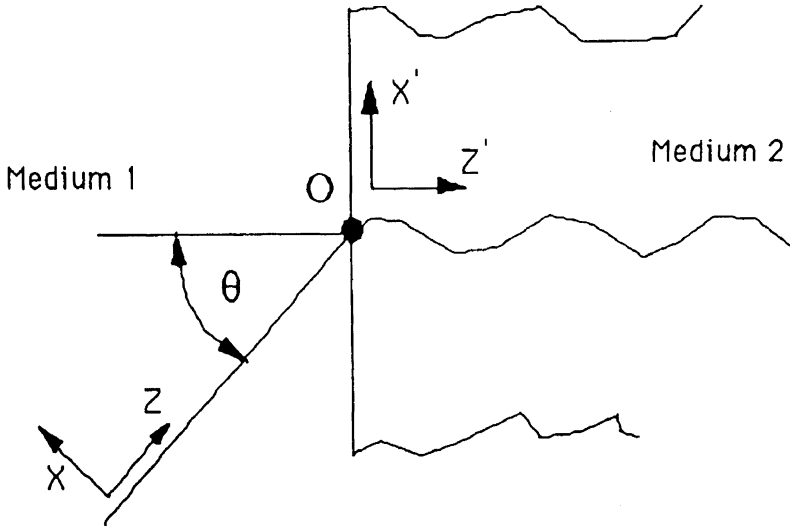


FIGURE 1: Schematic of the boundary between two media.

4 THE BODY OF THE PARALLEL FACE BEND

Consider a bending magnet that has Cartesian symmetry. We want to use Cartesian coordinates to integrate the orbit inside the magnet. The Hamiltonian for this magnet is given by:

$$H = H_1 + H_2$$

$$H_1 = -\sqrt{(1 + \delta)^2 - p_x^2 - p_y^2} + b_0 x$$

$$H_2 = V(x, y, \rho_c = \infty) . \quad (4.1)$$

According to our Lego-block formalism, the full map M for the parallel-face bend displayed in Figure 2 is given by:

$$M = Y_{\text{rot}}\left(\frac{\theta}{2}\right) \text{Fringe}(1) M_{//} \text{Fringe}(2) Y_{\text{rot}}\left(\frac{\theta}{2}\right) . \quad (4.2)$$

Approximate fringe maps, which account for mainly vertical focusing, are discussed in Appendix A.

The map $M_{//}$ is obtained by symplectic integration of H_1 and H_2 . The map for H_1 , which propagates a particle a distance z along the $z_1 - z_2$ axis is obtained from the sector bend by a limiting process:

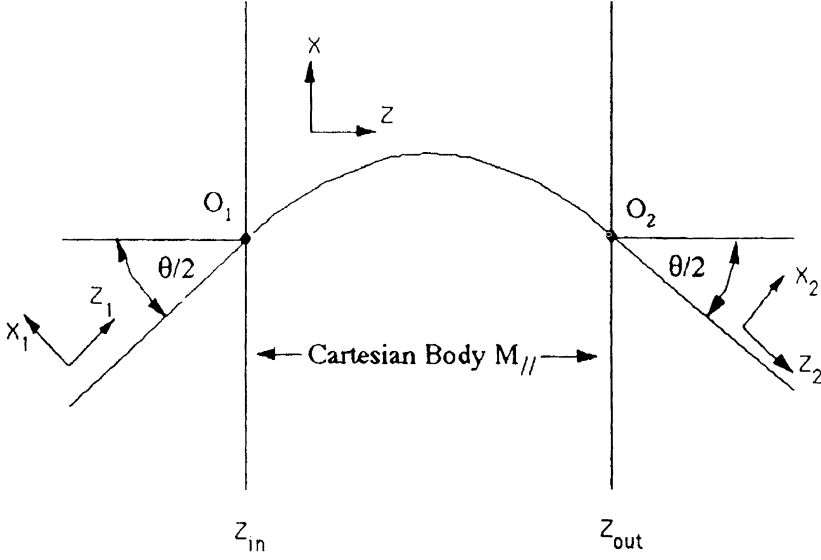


FIGURE 2: Parallel-face bend whose full map is given by Equation (4.2).

$$\exp(-z : H_1 :) = P(z, b_0) = \lim_{\substack{\rho_c \rightarrow \infty; \theta \rightarrow 0 \\ \rho_c \theta = z}} S(z, \rho_c, b_0) . \quad (4.3)$$

The limit is given by the formulae:

$$x^f = x + \frac{1}{b_0} \left\{ \sqrt{(1 + \delta)^2 - p_x^{f2} - p_y^2} - \sqrt{(1 + \delta)^2 - p_x^2 - p_y^2} \right\}$$

$$p_x^f = p_x - b_0 z$$

$$y^f = y + \frac{p_y}{b_0} \left\{ \arcsin \left(\frac{p_x}{\sqrt{(1 + \delta)^2 - p_y^2}} \right) - \arcsin \left(\frac{p_x^f}{\sqrt{(1 + \delta)^2 - p_y^2}} \right) \right\}$$

$$\tau^f = \tau + \frac{(1 + \delta)}{b_0} \left\{ \arcsin \left(\frac{p_x}{\sqrt{(1 + \delta)^2 - p_y^2}} \right) - \arcsin \left(\frac{p_x^f}{\sqrt{(1 + \delta)^2 - p_y^2}} \right) \right\} . \quad (4.4)$$

Finally, we point out that in order to automatically preserve the Lego block when dealing with ideal bends (no vector potential), we use $P \left(z, b_0 = \frac{1}{\rho_c} \right)$ in the symplectic integrator,

where ρ_c refers to the ideal arc of circle connecting the entrance and exit surface of the block. Any fluctuation in the bending field is included in the vector-potential part.

5 THE TWO TYPES OF GENERAL BENDS

5.1 *The Cylindrically Symmetric Bend*

In the case of a combined function bend with cylindrical symmetry but arbitrary entrance and exit angles, the body of the bend must be represented by a sector bend map. Cylindrical geometry implies that an easy solution of Maxwell's equations in the body is found in cylindrical coordinates. One gets the famous feed-up terms proportional to inverse powers¹⁹ of ρ_c in the vector potential of Equation (2.1). Then the following decomposition is possible:

$$\begin{aligned} \text{Map}(\theta) &= Y_{\text{rot}}(\alpha_1) \text{Fringe}(1) \text{Body}(\theta) \text{Fringe}(2) Y_{\text{rot}}(\alpha_2) \\ \text{Body}(\theta) &= Y_{\text{rot}}^F(-\alpha_1) M_{\angle}(\theta) Y_{\text{rot}}^F(-\alpha_2) . \end{aligned} \quad (5.1)$$

As shown in Figure 3, the map $Y_{\text{rot}}^F(\alpha)$ is a rotation of angle α (at the point of entry or exit) in the medium of the combined function bend. In the absence of real knowledge about the nature of the fringe-field region, the constant-field expression of Equation (3.2) can be used for $Y_{\text{rot}}^F(\alpha)$, and any correction to this map can be lumped in the maps Fringe (1) and Fringe (2) as we will discuss in Section 6.

Usually, approximate values of Fringe (1) and Fringe (2) are obtained by solving Maxwell's at the boundary to first order (see Appendix A and Reference 20).

5.2 *The Translationally Invariant Bend*

Finally, if the bend has rectangular symmetry, like a shifted quadrupole, the same technique can be used (see Figure 4).

$$\begin{aligned} \text{Map}(\theta) &= Y_{\text{rot}}(\alpha_1) \text{Fringe}(1) \text{Body}(\theta) \text{Fringe}(2) Y_{\text{rot}}(\alpha_2) \\ \text{Body}(\theta) &= Y_{\text{rot}}^F\left(\frac{\theta}{2} - \alpha_1\right) M_{//}(\theta) Y_{\text{rot}}^F\left(\frac{\theta}{2} - \alpha_2\right) . \end{aligned} \quad (5.4)$$

Again, the computation of the exact potential term is a bit tricky when the bend is not ideal and it can be lumped into the fringe maps.

We now continue with the second part of this article: the topic of fringe fields and misalignments.

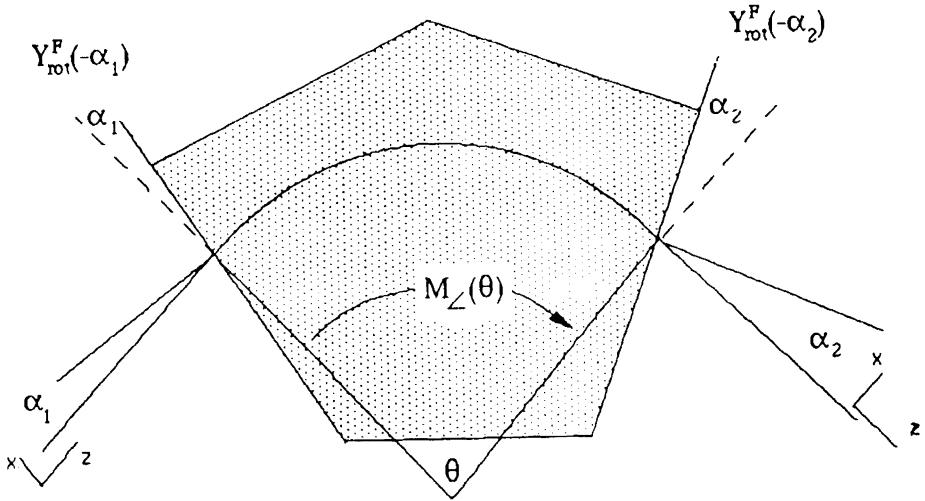


FIGURE 3: Geometry of a bend with cylindrical symmetry.

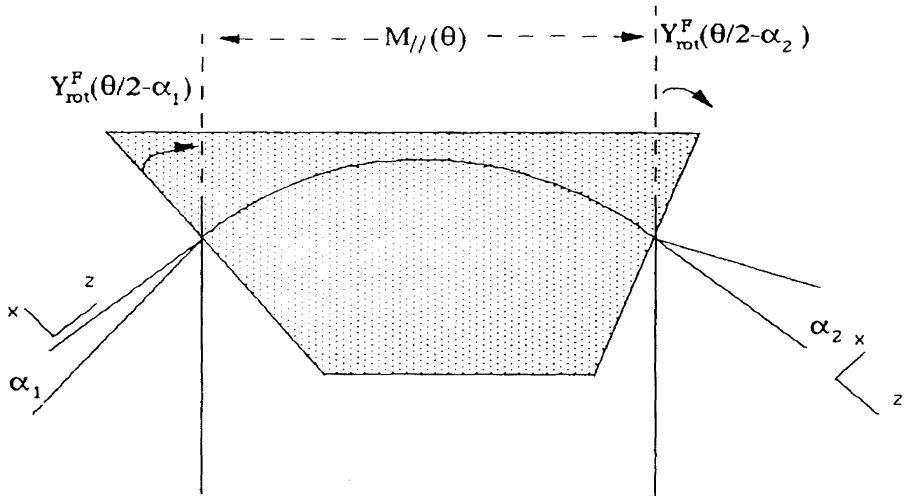



Figure 4
 Bend Medium = 

FIGURE 4: Geometry of a bend with rectangular symmetry (translational invariance).

6 THE FRINGE FIELD ISSUE

6.1 Zero-Length Fringe Field Insertions

In the simulation of circular rings, it is often possible to neglect fringe fields or to represent them by very simple models. For example, in Appendix A, we derive the approximate fringe map for bends. It provides vertical focusing and is therefore usually included in all simulations. These approximate fringe fields are obtained by solving Maxwell's equations to first order in the B-field and letting the length of the fringe field region go to zero. Hence they produce zero length maps.

However, we may be confronted with the need to compute a more realistic mapping for the fringe-field region. To the extent that we view this fringe as a perturbation of the ideal machine, it would be nice to insert this exact fringe map as a zero length map so that the structure of the lattice would be changed in a minimal way. In fact, zero length maps are Lego-block inserts that do not require any modification of the original lattice. To see how one may proceed, let us imagine the case of straight elements like a quadrupole of length L_Q preceded by a drift of length L_D . Let us suppose that the fringe field region extends from $z = -\varepsilon$ to $z = \varepsilon$, where $z = 0$ is the boundary of the ideal quadrupole.

For the ideal machine, the map describing motion from $z = -L_D$ to the center of the quadrupole is given by:

$$M = \text{Drift}(L_D) \text{Quad}(L_Q/2) . \quad (6.1)$$

Under the assumption $\varepsilon < L_Q/2$, the realistic map is just:

$$M_F = \text{Drift}(L_D - \varepsilon) \text{Fringe Quad}(L_Q/2 - \varepsilon) . \quad (6.2)$$

How can we make M_F look like Equation (6.1) as much as possible? We simply introduce inverse drifts and inverse quadrupoles:

$$\begin{aligned} M_F &= \text{Drift}(L_D) \{ \text{Drift}(-\varepsilon) \text{Fringe Quad}(-\varepsilon) \} \text{Quad}(L_Q/2) \\ &= \text{Drift}(L_D) I_f \text{Quad}(L_Q/2) \end{aligned}$$

where I_f is the zero length insertion

$$I_f = \text{Drift}(-\varepsilon) \text{Fringe Quad}(-\varepsilon) . \quad (6.3)$$

With this simple idea, we can modify an ideal ring with exact fringe-field maps without touching its basic structure, i.e., the Lego blocks of Reference 5. Of course, if fringe fields are omnipresent and omnipotent, there is little advantage in using zero length insertions.

6.2 Computing the Fringe Field Map

6.2.1 Numerical Integration of the Ray

There is always numerical integration. However, the theory of explicit symplectic integration does not apply because the Hamiltonian is not separable into exactly solvable parts. We must either use a higher-order ordinary integrator or use an implicit symplectic integrator. Recent advances in the theory of symplectic integration by Forest *et al*¹⁷ have allowed formulae used in explicit integration to be used to generate implicit integrators. In some of our codes, we have opted for a sixth-order non-symplectic Runge-Kutta method.

6.2.2 Automatic Differentiation Techniques

Using an automatic differentiation package, one can directly integrate the Taylor series through the fringe field. Many ways are available, depending on the degree of accuracy needed. For a circular machine, we generally discourage the use of the Taylor series for tracking. Nevertheless, the integration methods described in Section 6.2.1 must all be equipped with automatic differentiation for the extraction of Taylor series maps for their subsequent analysis.

A final comment: the creation of a zero length insertion is harder for the fringe fields of bend blocks. The topic of the next section is closely connected to its solution. We encourage the reader to read Section 7 and reproduce for a bend magnet the construction done in Section 6.1 for a quadrupole.

7 MISPLACEMENTS AND MISALIGNMENTS OF A MAGNET

To account for the misalignment of an element in a general way, one needs the full Euclidean group. In other words, we need rotations in the plane perpendicular to the direction of propagation, the horizontal Y_{rot} of Equation (2.3), and a vertical X_{rot} which is the same as Y_{rot} with x and y interchanged. We also need translations in the three spatial directions. We assume that the element is immersed in a field-free environment.

Normally, these operations will be performed in a Cartesian frame for simplicity. This is only a problem in a bend. Here a bend is defined as an element for which we elected to change the orientation of the reference coordinates, i.e., the Lego-bend block of Reference 5. This is depicted in Figure 5: the frame of reference is rotated by a total angle of θ from entrance to exit. Our Cartesian frame is obtained by rotating in the $x - z$ plane by $\theta/2$ at the entrance and at the exit.

$$M = Y_{\text{rot}} \left(\frac{\theta}{2} \right) M_c Y_{\text{rot}} \left(\frac{\theta}{2} \right) \quad (7.1)$$

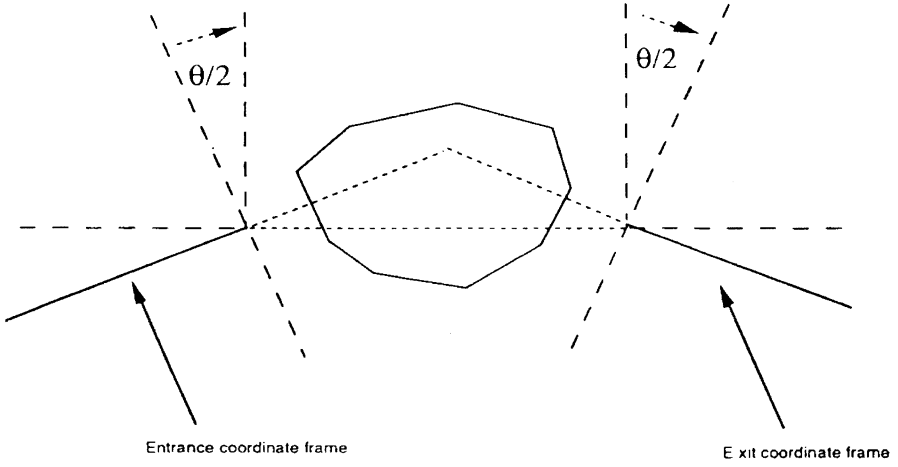


FIGURE 5: Making a bend block into a straight block.

In the Cartesian frame of Figure 5, it is very easy to apply a transverse rotation or translation. We start by defining the operators associated with these misalignments.

First, we define Z_{rot} : it is simply a transverse rotation. It is generated by the Lie exponent L_z :

$$\mathbf{w}^f = Z_{\text{rot}}(\alpha)\mathbf{w} = \exp(:\alpha L_z :) \mathbf{w} \quad \text{where } L_z = xp_y - yp_x \quad (7.2)$$

or, in component form,

$$\begin{aligned} x^f &= \cos(\alpha)x + \sin(\alpha)y \\ p_x^f &= \cos(\alpha)p_x + \sin(\alpha)p_y \\ y_f &= -\sin(\alpha)x + \cos(\alpha)y \\ p_y^f &= -\sin(\alpha)p_x + \cos(\alpha)p_y \\ \tau^f &= \tau \quad \text{and} \quad \delta^f = \delta. \end{aligned} \quad (7.3)$$

In this same transverse plane, we define the transverse translation $T(\mathbf{d}')$:

$$\mathbf{w}^f = T(\mathbf{d}')\mathbf{w} = \exp(:d_x p_x + d_y p_y :) \mathbf{w}$$

or

$$x_f = x - d_x \quad \text{and} \quad y^f = y - d_y \quad (7.4)$$

Finally we define longitudinal translations. If the element to be misaligned is embedded in a field-free region then we are dealing with drifts. Hence a translation by d_z is given by:

$$\begin{aligned}
 T(d_z)\mathbf{w}^f &= \exp(: d_z \sqrt{(1+\delta)^2 - p_x^2 - p_y^2} :) \mathbf{w} \\
 x^f &= x + d_z \frac{p_x}{\sqrt{(1+\delta)^2 - p_x^2 - p_y^2}} \quad y^f = y + d_z \frac{p_y}{\sqrt{(1+\delta)^2 - p_x^2 - p_y^2}} \\
 \tau^f &= \tau + d_z \frac{(1+\delta)}{\sqrt{(1+\delta)^2 - p_x^2 - p_y^2}}. \tag{7.5}
 \end{aligned}$$

Because of the commutation of the various Lie exponents, the general translation in field-free regions is just:

$$T(\mathbf{d}) = \exp(: d_x p_x + d_y p_y + d_z \sqrt{(1+\delta)^2 - p_x^2 - p_y^2} :) . \tag{7.6}$$

Noticed that $\sqrt{(1+\delta)^2 - p_x^2 - p_y^2}$ is just p_z which accidentally gives to Equation (7.6) the expected symmetry:

$$T(\mathbf{d}) = \exp(: d_x p_x + d_y p_y + d_z p_z :) = \exp(: d_x p_x + d_y p_y - d_z H :) . \tag{7.7}$$

The fact that a z translation corresponds to propagation within the medium is self-evident. Clearly, in general, $T(d_z)$ is just the time ordered exponential $Texp\left(\int_{z_0}^{z_0+d_z} : -H : \right)$ and does not commute with the transverse translations. It commutes only within a field-free (drift) region

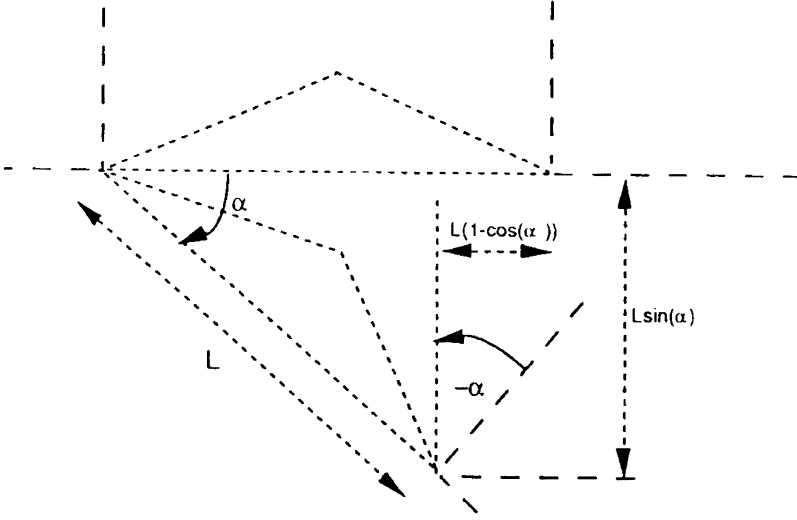
For all the operations described above, it is correct to say that the displaced element is given by the map

$$M_c(E) = EM_cE^{-1}, \tag{7.8}$$

where E is the map of the displacement (i.e., a product of the operations we just defined) and M_c is the map of the element in the Cartesian frame of Figure 5.

Our job is almost complete. We have only the $x-z$ and $y-z$ rotations left. Unfortunately, they are more complicated and more subtle to apply to an element. Strangely enough, Equation (7.8) does not apply to them because they mix the transverse directions with the direction of propagation. It turns out that Equation (7.8) does apply to Y_{rot} and X_{rot} , if and only if, the element represented by M has zero length. Before exploiting this property, let us work out a special case using geometrical considerations.

Let us start with a simple example: a rotation of angle α in the $x-z$ plane about the entry point of the reference orbit. It is simply $Y_{\text{rot}}(\alpha)$. The question is: what is the equivalent of Equation (7.8) when the whole element is rotated about the entry point around the y axis by an angle α ? This is best answered by looking at Figure 6.

FIGURE 6: Geometry of x - z rotation.

In Figure 6 the magnet is rotated at the entrance around the origin of the reference frame, i.e., $Y_{\text{rot}}(\alpha)$. Then a ray propagates through the magnet (M_c). Finally, the ray must be brought back to the original frame for further propagation through the lattice as demanded by the Lego-block formalism. This is done by $Y_{\text{rot}}(-\alpha)$, followed by an x translation of $L \sin(\alpha)$ and finally by a z translation (i.e., drift) of $L(1 - \cos(\alpha))$.

Notice that all the additional maps introduced in Figure 6 depend on the length L of the element being rotated. So, following our observation for thin elements, in a way similar to the section on the fringe field, we make the element thin at the rotation point (which here is the entry point $d = 0$):

$$M_c = \text{Drift}(d) M_{\text{thin}} \text{Drift}(L - d)$$

$$M_{\text{thin}} = \text{Drift}(-d) M_c \text{Drift}(-L + d) . \quad (7.9)$$

In Equation (7.9) the map M_{thin} is a zero length insertion located at a distance d from the entrance.

We now rotate the thin element by an angle α .

$$M_c(\alpha; d) = \text{Drift}(d) Y_{\text{rot}}(\alpha) M_{\text{thin}} Y_{\text{rot}}(-\alpha) \text{Drift}(L - d) . \quad (7.10)$$

Of course, the special example of Figure 6 is gotten by setting d to zero:

$$\begin{aligned} M_c(\alpha; 0) &= Y_{\text{rot}}(\alpha) M_{\text{thin}} Y_{\text{rot}}(-\alpha) \text{Drift}(L) \\ &= Y_{\text{rot}}(\alpha) M_c \text{Drift}(-L) Y_{\text{rot}}(-\alpha) \text{Drift}(L) . \end{aligned} \quad (7.11)$$

Using some standard properties of the Lie exponents, we can move the operators of Equation (7.11) into an order compatible with the operations described in Figure 6.

$$\begin{aligned}
 M_c(\alpha; 0) &= Y_{\text{rot}}(\alpha) M_c \text{Drift}(-L) Y_{\text{rot}}(-\alpha) \text{Drift}(L) \\
 &= Y_{\text{rot}}(\alpha) M_c Y_{\text{rot}}(-\alpha) Y_{\text{rot}}(\alpha) \text{Drift}(-L) Y_{\text{rot}}(-\alpha) \text{Drift}(L) \\
 &= Y_{\text{rot}}(\alpha) M_c Y_{\text{rot}}(-\alpha) \exp\left(L : Y_{\text{rot}}(\alpha) \sqrt{(1 + \delta)^2 - p_x^2 - p_y^2} : \right) \text{Drift}(L) \\
 &= Y_{\text{rot}}(\alpha) M_c Y_{\text{rot}}(-\alpha) \\
 &\quad \exp\left(L : \sqrt{(1 + \delta)^2 - \left(\cos(\alpha) p_x + \sin(\alpha) \sqrt{(1 + \delta)^2 - p_x^2 - p_y^2}\right)^2 - p_y^2} \right. \\
 &\quad \left. - \sqrt{(1 + \delta)^2 - p_x^2 - p_y^2} : \right) . \tag{7.12}
 \end{aligned}$$

One can show that the last factor in Equation (7.12) is just one of the operators of Figure 6. In fact, from Figure 6, we deduce that

$$\begin{aligned}
 M_c(\alpha; 0) &= Y_{\text{rot}}(\alpha) M_c Y_{\text{rot}}(-\alpha) \exp(: L \sin(\alpha) p_x :) \exp(L : (1 - \cos(\alpha)) \\
 &\quad \sqrt{(1 + \delta)^2 - p_x^2 - p_y^2} :) \\
 &= Y_{\text{rot}}(\alpha) M_c Y_{\text{rot}}(-\alpha) \exp(L : p_x \cos(\alpha) + (1 - \cos(\alpha)) \\
 &\quad \sqrt{(1 + \delta)^2 - p_x^2 - p_y^2} :) . \tag{7.13}
 \end{aligned}$$

It is a simple exercise in algebra to verify that Equations (7.12) and (7.13) are identical.

As an example of the proper usage of these maps, let us rotate and translate a general non-ideal bend of bending angle θ around its median plane. The bend, without misalignments, is described the map $M(\theta)$. This map could be arbitrarily complex.

We start by going into Cartesian coordinate (Figure 5):

$$M_c = Y_{\text{rot}}\left(-\frac{\theta}{2}\right) M Y_{\text{rot}}\left(-\frac{\theta}{2}\right) . \tag{7.14}$$

Next we turn it into a thin lens at location $d = \frac{L}{2}$:

$$M_{\text{thin}}(\theta) = \text{Drift}\left(-\frac{L}{2}\right) M_c(\theta) \text{Drift}\left(-\frac{L}{2}\right) . \tag{7.15}$$

Then we misalign the element by a transformation of the Euclidean group denoted by E :

$$M_{\text{thin},E}(\theta) = EM_{\text{thin}}(\theta)E^{-1} . \quad (7.16)$$

The map E is an arbitrary product of the transformations we have just introduced:

$$E = \prod_i E_i ,$$

where

$$E_i \in \{Z_{\text{rot}}, X_{\text{rot}}, Y_{\text{rot}}, T(\mathbf{d})\} . \quad (7.17)$$

Finally, the map must be restored to its normal frame:

$$M_E(\theta) = Y_{\text{rot}}(\theta/2) \text{Drift}\left(\frac{L}{2}\right) M_{\text{thin},E}(\theta) \text{Drift}\left(\frac{L}{2}\right) Y_{\text{rot}}(\theta/2) . \quad (7.18)$$

The operations of this section require the creation of a thin element at the center of the Lego-block. This is done using $Y_{\text{rot}}(\theta/2)$. The reader will notice that this map diverges at $\theta = 180$ degrees. This implies that we cannot use the method of this section to move an element which bends the beam by an angle near 180 degrees. This problem can be solved by turning such an element into a 180 degrees block using the appropriate Y_{rot} . Then, using a modified theory, the operators in Equation (7.17) can be used to move this type of element. This theory has been worked out and will be published.

8 INCLUSION OF CLASSICAL RADIATION AND THE STOCHASTIC EFFECTS IN THE ULTRA-RELATIVISTIC REGIME

In an electron ring, the final beam sizes are the results of a balance between the natural damping of a non-symplectic system and the diffusion due to a stochastic process induced by the granularity of the photon emission. In small or large rings, it would be nice to introduce these effects in a completely self-consistent way. This task is divided into two parts:

- (1) the inclusion of a classical radiating particle ($\hbar = 0$), and
- (2) the computation of the stochastic diffusion.

There are three basic approaches to the problem, which we list in order of increasing exactness:

- (1) Sand's formulation: good for small damping and no dispersion at the cavity.
- (2) Chao's 6-d synchrotron integrals: good for small damping.
- (3) Beam envelope calculation: good all the time provided the beam occupies a linear region around the synchronous orbit and of course, always at least as good as the

two previous approaches. To our knowledge this approach was first suggested by Ruggiero¹¹ and has been used in the code `SAD`.¹⁸

It is worth mentioning that Sand's and Chao's formalisms can fall apart near linear resonances. This is very unsettling when considering the design and study of low momentum-compactness (quasi-isochronous) machines. To be more precise, if the distance in tune from a resonance is on the order of the damping, the synchrotron integral formalism breaks down. The concept of equilibrium emittance is totally nonsensical. This could be of some relevance in studies of a beam away from equilibrium (beam-beam interaction, for example).

In this paper, we describe primarily the beam envelope formalism. In Appendix B, we present the Chao integral formalism and its connection with the beam-envelope treatment of this section.

8.1 Classical Radiation

We start with the classical radiation, following closely an approach originally due to Chao.¹² According to Sands,²¹ the change in the fifth variable δ due to radiation is obtainable from the formula:

$$\frac{d\delta}{dt} = -K(1 + \delta)^2 \left(\frac{\mathbf{B}_\perp}{B_\rho} \right)^2 ; \quad K = 1.40789357 \cdot 10^{-5} E_0^3 .$$

$$\text{where the design energy } E_0 \text{ is in GeV} \quad (8.1)$$

Here \mathbf{B}_\perp is the component of the magnetic field perpendicular to the direction of propagation.

Knowing the coordinate frame used (either Cartesian or cylindrical in this paper), one can easily derive \mathbf{B}_\perp from the formula:

$$\mathbf{B}_\perp = \mathbf{B} \times \mathbf{e} , \quad (8.2)$$

where \mathbf{e} is a unit vector in the direction of propagation. The magnetic field is obtained from the equation of motion of the underlying symplectic system.

The other piece of physics one introduces is the conservation of \mathbf{e} in the ultra-relativistic regime. The canonical variables p_x and p_y are not preserved, but $\frac{dx}{ds}$ and $\frac{dy}{ds}$ are conserved. Putting everything together, we obtain the following formulae for a time step (i.e., ds step) of the modified symplectic integrator:

$$\Delta = \delta^f - \delta = K(1 + \delta)^2 \frac{\mathbf{B}_\perp^2}{(B_\rho)} \frac{\partial H}{\partial \delta} ds \quad (8.3a)$$

$$\frac{\left(p_x^f - a_x, p_y^f - a_y \right)}{\sqrt{(1 + \delta - \Delta)^2 - (\mathbf{p}^f - \mathbf{a})^2}} = \frac{\left(p_x - a_x, p_y - a_y \right)}{\sqrt{(1 + \delta)^2 - (\mathbf{p} - \mathbf{a})^2}} \quad (8.3b)$$

$$d\tau = -\frac{\partial H}{\partial \delta} ds \quad \text{and} \quad \mathbf{a} = \frac{(A_x, A_y)}{(B_\rho)} \quad (8.3c)$$

Equation (8.3b) is valid in Cartesian as well as cylindrical coordinates. As implied by Equation (8.3), the motion of the particle will no longer be consistent with the symplectic condition. In fact, if a new closed orbit $\mathbf{w}_{r_0}(s)$ is found, the map around it will have the following properties:

$$w_{\text{total}i}^f = w_{r_0i} + w_i^f = w_{r_0i} + T_{ij}^1 w_j + T_{ijk}^2 w_j w_k + \dots \quad (8.4a)$$

$$\mathbf{w} = (x, p_x, y, p_y, \delta, \tau), \quad (8.4b)$$

where the eigenvalues of T^1 are given by

$$\lambda_{\pm k} = \exp(-\alpha_k \pm i2\pi\nu_k) \quad ; \quad k = 1, 2, 3. \quad (8.5)$$

The constants α_k are the damping coefficients of the map. It is noteworthy that this particular calculation is valid even in the presence of a large radiative coefficient K and is fully six-dimensional. By contrast, the approach of Sands is restricted and assumes no dispersion at the cavities.

In general, since the damping coefficients are very small and the map is nearly symplectic, it is important that the original integrator be symplectic to an accuracy at least a couple of orders of magnitude smaller than the natural non-symplectic effects of radiation. Here, for the ideal machine, the integrator is exactly symplectic. For the fringe-field regions, it is advisable to use a high order method to ensure symplecticity of the original map.

For the stochastic effects, we used the beam-envelope formalism.

8.2 Stochastic Diffusion: Computation of the Beam Envelopes

Here we will concentrate on the linear part of the map. Since the purpose of this section is to find the equilibrium beam sizes, it will be assumed that the final beam sizes are small compared to the dynamic aperture (more precisely, to sizes within the region where the linear approximation is valid).

We start by defining the second-order moments:

$$\Sigma_{ij}(s) = \langle v_i(s)v_j(s) \rangle \quad \text{where} \quad \mathbf{v} = \left(x, \frac{dx}{ds}, y, \frac{dy}{ds}, \delta, \tau \right). \quad (8.6)$$

This vector \mathbf{v} is defined around the radiative closed orbit^h $\mathbf{v}_{r_0}(s)$ found in the previous subsection. The computation of the matrix Σ is trivial with automatic differentiation. It requires us to know \mathbf{w}_{r_0} at every integration step and the expression connecting $\left(\frac{dx}{ds}, \frac{dy}{ds} \right)$ to (p_x, p_y) , i.e., connecting \mathbf{w}_{r_0} to \mathbf{v}_{r_0} . This expression is directly available from the

^h The beam envelope ϵ and the diffusion matrix B , which we later define, make sense around any orbit. They are local concepts. Here, we separated the search of the closed orbit and the computation of ϵ only for reasons of clarity.

Hamiltonian. From now on we assume that the particle distribution is described by a Gaussian.

Let us assume that the particle's energy undergoes a small fluctuation Δ during a time interval dt . Because of the conservation of $\left(\frac{dx}{ds}, \frac{dy}{ds}\right)$ during this process, we get:

$$\Sigma_{ij}^f(s) = \Sigma_{ij}(s) + dB_{ij}; \quad dB_{55} = \langle \Delta^2 \rangle \quad \text{is the only nonzero component.} \quad (8.7)$$

Using quantum mechanics for $\langle \Delta^2 \rangle$,²¹ we get the final expression of dB_{55} :

$$\begin{aligned} dB_{55} &= K'(1 + \delta)^4 \left| \frac{\mathbf{B}_\perp}{B_\rho} \right|^3 d\tau \\ &= -K'(1 + \delta)^4 \left| \frac{\mathbf{B}_\perp}{B_\rho} \right|^3 \frac{\partial H}{\partial \delta} ds \\ K' &= 4.13209717 \cdot 10^{-11} E_0^5 \end{aligned}$$

$$\text{where the design energy } E_0 \text{ is in GeV.} \quad (8.8)$$

Of course we must relate the diffusion at one location s to the origin $s = 0$ which is our point of observation. Notice that we express the diffusion matrix at $s = 0$ using canonical variables (i.e., \mathbf{w}). The matrix \hat{T} connects canonical variables at $s = 0$ to noncanonical variables at s :

$$\begin{aligned} dB_{ij}(s) &= \langle v_i(s)v_j(s) \rangle = \left\langle \hat{T}_{ia}(0 \rightarrow s) \hat{T}_{jb}(0 \rightarrow s) w_a(0)w_b(0) \right\rangle \\ &= \hat{T}_{ia}(0 \rightarrow s) \hat{T}_{jb}(0 \rightarrow s) \langle w_i(0)w_j(0) \rangle \\ &= \hat{T}_{ia}(0 \rightarrow s) \hat{T}_{jb}(0 \rightarrow s) dB_{ij}(0), \end{aligned} \quad (8.9a)$$

or, in matrix language,

$$dB(s) = \hat{T}(0 \rightarrow s) dB(0), \quad \tilde{T}(0 \rightarrow s), \quad \tilde{T} \text{ means transposed of } T. \quad (8.9b)$$

Therefore the total diffusion matrix for one turn, expressed at $s = 0$ in canonical variables is given by:

$$B_{ij}^0 = \oint_{s=0}^{s=C} \hat{T}_{i5}^{-1}(0 \rightarrow s) \frac{dB_{55}}{ds} \tilde{T}_{5j}^{-1}(0 \rightarrow s) ds. \quad (8.10)$$

Here C is the circumference of the ring. The integral is really a sum over all the local integration steps in each Lego block.

The total matrix of moments Σ for one turn, is given by:

$$\begin{aligned}\Sigma^f &= T(0 \rightarrow C) \left\{ \Sigma^0 + B^0 \right\} \tilde{T}(0 \rightarrow C) \\ &= T(0 \rightarrow C) \Sigma^0 \tilde{T}(0 \rightarrow C) + B^f\end{aligned}\quad (8.11)$$

$$\text{where } B^f = T(0 \rightarrow C) B^0 \tilde{T}(0 \rightarrow C)$$

At equilibrium, the moments do not change during a turn; hence the equilibrium matrix Σ_∞ is given by the fixed point of Equation (8.11):

$$\Sigma_\infty = T(0 \rightarrow C) \Sigma_\infty \tilde{T}(0 \rightarrow C) + B^f \quad (8.12)$$

The operation $\hat{T} \Sigma \tilde{T}$ on a arbitrary vector of 21 components $\vec{\Sigma}$ can be represented by a matrix Θ :

$$\begin{aligned}\vec{\Sigma}_\infty &= \Theta \vec{\Sigma}_\infty + \vec{B}^f \Rightarrow \vec{\Sigma}_\infty = (1 - \Theta)^{-1} \vec{B}^f \\ &= -(1 - \Theta^{-1})^{-1} \vec{B}^0\end{aligned}\quad (8.13)$$

Of course, Σ_∞ contains the equilibrium beam sizes at $s = 0$ by construction:

$$\Sigma_{\infty;ij} = \langle w_i(0) w_j(0) \rangle . \quad (8.14)$$

9 CONCLUSION

We have introduced the bare minimum of knowledge required for the design of a simulation code appropriate for small rings. No complete job can be done without

- (1) A good understanding of the local (Lego) approach to particle tracking;
- (2) Maxwell's equations which are important in the fringe fields and in the body of sector bends;
- (3) automatic differentiation tools such as the original DA package of Berz;
- (4) Inclusion of radiative effects
- (5) A normal-form analysis package such as our own LIELIB, which include symplectic and non-symplectic normal forms to arbitrary order.

ACKNOWLEDGEMENTS

We would like to thank Lindsay Schachinger (LBL) and John Irwin (SLAC) for taking a serious look at this paper. Also we would like to thank Jim Murphy (BNL) and Claudio Pellegrini (UCLA) for providing actual small machine lattices on which to test these ideas. We acknowledge the help of David Robin (LBL) for the thin lens procedure of Section 7, and Johan Bengtsson (LBL). We are grateful to Drs. K. Ohmi, K. Hirata and K. Oide of KEK, who converted us to the beam-envelope formalism. A lot of the ideas presented in this paper have been used independently by the KEK group in their computer code SAD.¹⁸ Finally, we are grateful to Dr. Leo Michelotti (FNAL) for discussions on the physics and computer aspects of particle tracking.

APPENDIX A: APPROXIMATE FRINGE MAP IN A BEND

To derive the famous vertical focusing effect, we assume that in the mid-plane there is a vertical field $B(z)$. This can be generated by a vector potential A_z :

$$A_z = -xB(z) . \quad (\text{A1})$$

It is easy to check that A_z does not obey Maxwell's equation. In fact the z dependence of A_z implies the existence of A_x :

$$\frac{\partial^2}{\partial y^2} A_x + \frac{\partial^2}{\partial z^2} A_x = -\frac{d}{dz} B . \quad (\text{A2})$$

To leading order in the y -variable, the answer for A_x is:

$$A_x = -\frac{1}{2} \frac{d}{dz} B y^2 + O(y^4) . \quad (\text{A3})$$

We substitute this in Equation (4.1),

$$H = -\sqrt{(1 + \delta)^2 - (p_x - a_x)^2 - p_y^2} + b_0(z)x , \quad (\text{A4})$$

where

$$b_0(z) = \frac{qB(z)}{p_0}, \quad \frac{q}{p_0} = \text{Magnetic Rigidity}$$

$$a_x = \frac{q}{p_0} A_x . \quad (\text{A5})$$

Next we expand the Hamiltonian to first order in the \mathbf{B} -field:

$$H = -\sqrt{(1+\delta)^2 - p_x^2 - p_y^2} - \frac{p_x a_x}{\sqrt{(1+\delta)^2 - p_x^2 - p_y^2}} + b_0(z)x . \quad (\text{A6})$$

To first order, the map for the fringe field is given by:

$$\text{Fringe} = \exp(: f :)$$

$$\begin{aligned} f &= -\lim_{\Delta \rightarrow 0} \int_{-\Delta}^{\Delta} H dz = \frac{q}{p_0} \left(\lim_{\Delta \rightarrow 0} \int_{-\Delta}^{\Delta} \frac{dB}{dz} dz \right) \frac{-\frac{1}{2}y^2 p_x}{\sqrt{(1+\delta)^2 - p_x^2 - p_y^2}} \\ &= \pm b_0 \frac{-\frac{1}{2}y^2 p_x}{\sqrt{(1+\delta)^2 - p_x^2 - p_y^2}} . \end{aligned} \quad (\text{A7})$$

Here the \pm refers to the entrance (+) and exit (-) pole faces. The quantity b_0 is $b_0(z)$ evaluated at the center of the magnet. The Lie exponent f can be replaced to first order in b_0 by a characteristic function C which is exactly solvable:

$$C = \mathbf{q}^{\text{fin}} \cdot \mathbf{p}^{\text{ini}} + f(\mathbf{q}^{\text{fin}}, \mathbf{p}^{\text{ini}}) . \quad (\text{A8})$$

First-order maps for the multipole fringe fields can also be computed using similar concepts.^{22,18}

APPENDIX B: DIRECT COMPUTATION OF THE “EMITTANCES”

What follows, up to Equation (B11) was first proposed by Chao.¹²

We start by noticing that the linear matrix T^1 can be normalized as follows:ⁱ

$$T^1 = A \Lambda R A^{-1} \quad (\text{B1a})$$

$$\Lambda_{2k-1 \ 2k-1} = \Lambda_{2k \ 2k} = \exp(-\alpha_k) \quad k = 1, 2, 3 \quad (\text{B1b})$$

$$R = \text{usual phase space rotation of angles } 2\pi \nu_k . \quad (\text{B1c})$$

ⁱ This factorization is also possible for the nonlinear map near the origin. However, the convergence of the map A as a power series is slow because of the presence of small denominators in the damping α , which are necessary to remove tune shifts from the nonlinear map.

We can compute an emittance-like quantity using the matrix A :

$$\varepsilon_k = \sum_{i=0,1} \left(\sum_{j=1,6} A_{2k-i,j}^{-1} w_j \right)^2 \quad k = 1, 2, 3 \quad (\text{B2a})$$

$$\mathfrak{S}\varepsilon_k = \exp(-2\alpha_k)\varepsilon_k. \quad (\text{B2b})$$

In line^{*j*} (B2b) \mathfrak{S} is the functional map^{*k*} associated with the coordinate transformation defined by T^1 (denoted by T from now on). More precisely, if

$$\mathbf{w}^f = \zeta(\mathbf{w}) = T\mathbf{w}$$

then $\mathfrak{S}\varepsilon_k$ is defined as

$$(\mathfrak{S}\varepsilon_k)(\mathbf{w}) = (\varepsilon_k \circ \zeta)(\mathbf{w}) = \varepsilon_k(T\mathbf{w}). \quad (\text{B3})$$

In the case of small damping,²³ we can assume that the emittances are nearly invariant and that the equilibrium distributions will depend only on the values of the ε_k 's. In fact, we will show later that this follows from the beam-envelope treatment.

We start by rewriting the emittances as follows:

$$\varepsilon_k = \sum_{i=0,1} \left(B_{2k-i,j}^{-1} v_j \right)^2 \quad k = 1, 2, 3$$

$$\text{where } \mathbf{v} = \left(x, \frac{dx}{ds}, y, \frac{dy}{ds}, \delta, \tau \right). \quad (\text{B4})$$

The computation of the matrix B is trivial with automatic differentiation. It requires us to know A at every integration step and the expression connecting $\left(\frac{dx}{ds}, \frac{dy}{ds} \right)$ to (p_x, p_y) . This expression is directly available from the Hamiltonian. The matrix $A(s)$ at location s is gotten from $A(0)$ at $s = 0$ by the formula $A(s) = T(0 \rightarrow s)A(0)$. Here $T(0 \rightarrow s)$ is the linear map for the motion around the closed orbit from $s = 0$ to s . With automatic differentiation, this computation is as trivial as the computation of the transfer map itself. The matrix B is obtained by the formula $B(s) = \hat{T}(0 \rightarrow s)A(0)$, where $\hat{T}(0 \rightarrow s)$ is defined as the matrix connecting $\mathbf{w}(0)$ and $\mathbf{v}(s)$ as in Section 8.

Now let us assume that the particle undergoes a small fluctuation Δ during a time interval dt . Because of the conservation of $\left(\frac{dx}{ds}, \frac{dy}{ds} \right)$ during this process, we get:

^{*j*} We drop the summation over $j(\mathcal{D}1,6)$ from now on.

^{*k*} In this paper we overload the notation, confusing the matrices and their functional maps. Only T changes into \mathfrak{S} for clarity.

$$d\varepsilon_k = 2 \left(\sum_{i=0,1} B_{2k-i}^{-1} B_{2k-i-5}^{-1} \Delta v_j \right) + \sum_{i=0,1} \left(B_{2k-i-5}^{-1} \right)^2 \Delta^2 \quad (\text{B5})$$

Because $\langle \Delta \rangle$ vanishes, we are left with:

$$d\varepsilon_k = \left\{ \sum_{i=0,1} \left(B_{2k-i-5}^{-1} \right)^2 \right\} \langle \Delta^2 \rangle_{\text{photon}} \quad (\text{B6})$$

Using quantum mechanics for $\langle \Delta^2 \rangle_{\text{photon}}$ as in Equation (8.8), we get the final expression of $d\varepsilon_k$:

$$\begin{aligned} d\varepsilon_k &= \left\{ \sum_{i=0,1} \left(B_{2k-i-5}^{-1} \right)^2 \right\} K' (1 + \delta)^4 \left| \frac{\mathbf{B}_\perp}{B_\rho} \right|^3 d\tau \\ &= \left\{ \sum_{i=0,1} \left(B_{2k-i-5}^{-1} \right)^2 \right\} K' (1 + \delta)^4 \left| \frac{\mathbf{B}_\perp}{B_\rho} \right|^3 \frac{\partial H}{\partial \delta} ds \\ &= \left\{ \sum_{i=0,1} \left(B_{2k-i-5}^{-1} \right)^2 \right\} \frac{dB_{55}}{ds} ds \end{aligned}$$

$$K' = 4.13209717 \cdot 10^{-11} E_0^5$$

$$\text{where the design energy } E_0 \text{ is in GeV ,} \quad (\text{B7})$$

The total change $\Delta\varepsilon_k$ for one turn around the ring is given by the integral of $d\varepsilon_k$.

$$\Delta\varepsilon_k = \oint d\varepsilon_k = \oint \left\{ \sum_{i=0,1} \left(B_{2k-i-5}^{-1} \right)^2 \right\} \frac{dB_{55}}{ds} ds . \quad (\text{B8})$$

The equilibrium emittances, which happen to be the mean emittances, are just:

$$\langle \varepsilon_k \rangle = \frac{1}{2\alpha_k} \Delta\varepsilon_k . \quad (\text{B9})$$

In the literature, the emittances (normalized beam sizes) are defined as half the mean emittances:

$$\sigma_k^2 = \frac{1}{2} \langle \varepsilon_k \rangle = \frac{1}{4\alpha_k} \Delta\varepsilon_k . \quad (\text{B10})$$

Beam sizes are gotten trivially using the transformation A:

$$\langle v_i^2 \rangle^{1/2} = \left(\sum_{k=1}^3 (A_{i2k-1}^2 + A_{i2k}^2) \sigma_k^2 \right)^{1/2}. \quad (\text{B11})$$

Now, we would like to connect this treatment with the more exact beam envelope approach of Section 8.

In Equation (B3) we introduced the functional map \mathfrak{S} associated to the matrix T . Since perturbation theory on maps involves functional maps (see Reference 5), we would like to transform Equation (8.12) into an equation involving functional maps.

To do this, we must construct a function with the moments Σ_{ij} . The choice is pretty obvious: $\sigma(\mathbf{w}) = \Sigma_{ij} w_i w_j$. Now, let us transform the function σ by the map $\tilde{\mathfrak{S}}$ associated to the matrix \tilde{T} :

$$(\tilde{T}\sigma)(\mathbf{w}) = \sigma(\tilde{T}\mathbf{w}) = \Sigma_{ij} \tilde{T}_{ia} w_a \tilde{T}_{jb} w_b = (T\Sigma\tilde{T})_{ij} w_i w_j \quad (\text{B12})$$

Equation (B12) demonstrates that σ transforms^l under the functional operator $\tilde{\mathfrak{S}}$ like Σ does under T . Hence, the equation for the function Σ which is mathematically equivalent to Equation (8.11) is:

$$\sigma^f = \tilde{\mathfrak{S}}\sigma + b^f = \tilde{\mathfrak{S}}(\sigma + b^0). \quad (\text{B13})$$

Here b^f is defined in the obvious way in terms of the diffusion matrix B^f :

$$b^f(\mathbf{w}) = B_{ij}^f w_i w_j \quad (\text{B14})$$

Following the theory of map diagonalization and Equation (B1), it is clear that the map associated with \tilde{A} , which we call \tilde{A}^{-1} , will diagonalize $\tilde{\mathfrak{S}}$.

$$\tilde{A}^{-1}\tilde{\mathfrak{S}}\tilde{T} = \tilde{R}\tilde{\Lambda} \quad (\text{B15})$$

We apply Equation (B15) to Equation (B13):

$$\begin{aligned} \tilde{A}^{-1}\sigma^f &= \tilde{A}^{-1}\tilde{\mathfrak{S}}\tilde{A}\tilde{A}^{-1}\sigma + \tilde{A}^{-1}b^f \\ &= \tilde{A}^{-1}\tilde{\mathfrak{S}}\tilde{A} \left(\tilde{A}^{-1}\sigma + \tilde{A}^{-1}b^0 \right) \\ \Rightarrow \sigma_n^f &= \tilde{R}\tilde{\Lambda}\sigma_n + b_n^f \\ &= \tilde{R}\tilde{\Lambda} \left(\sigma_n + b_n^0 \right) \end{aligned} \quad (\text{B16})$$

^l The moments space is dual to the function space.

Here the subscript “n” refers to the “normalized” value of the functions. Again we are looking for a fixed point solution of Equation (B16). As in Equation (8.13), the solution is

$$\Rightarrow \sigma_{n;\infty} = \left(1 - \tilde{R}\tilde{\Lambda}\right)^{-1} b_n^f = - \left\{1 - \left(\tilde{R}\tilde{\Lambda}\right)^{-1}\right\}^{-1} b_n^0. \quad (\text{B17})$$

To proceed further we rewrite b_n^0 in terms of the quantities in Equation (8.10)

$$b_n^0 = \oint_{s=0}^{s=C} \tilde{A}^{-1} \tilde{\mathfrak{S}}^{-1}(0 \rightarrow s) \sigma_\delta \frac{dB_{55}}{ds} ds$$

$$\sigma_\delta \text{ is defined as } \forall \mathbf{w} \quad \sigma_\delta(\mathbf{w}) = w_5^2 = \delta^2 \quad (\text{B18})$$

This expression must be compared to $d\varepsilon_k$ of Equation (B6). To do this, we first realize that the matrix associated with $\tilde{A}^{-1} \tilde{\mathfrak{S}}^{-1}(0 \rightarrow s)$ is \tilde{B}^{-1} , and here is the one-line proof:

$$B = \hat{T}(0 \rightarrow s)A(0) \Rightarrow \tilde{B} = \tilde{A}(0)\tilde{T}(0 \rightarrow s)$$

$$\Rightarrow \tilde{B}^{-1} \tilde{T}^{-1}(0 \rightarrow s) \tilde{A}^{-1}(0) \xrightarrow{\text{for functional maps}} \tilde{B}^{-1} = \tilde{A}^{-1}(0) \tilde{\mathfrak{S}}^{-1}(0 \rightarrow s) \quad (\text{B19})$$

We now put this result in (B18):

$$b_n^0(\mathbf{w}) = \oint_{s=0}^{s=C} \left\{ \sum_{i=1}^6 B_{i5}^{-1} w_i \right\}^2 \frac{dB_{55}}{ds} ds \quad (\text{B20})$$

The final step requires a resonance basis analysis of Equation (B20). We notice that the functional map $\tilde{R}\tilde{\Lambda}$ is diagonal in the famous resonance basis:

$$\sigma_{km\varepsilon_k\varepsilon_m}(\mathbf{w}) = (q_k + i\varepsilon_k p_k) (q_m + i\varepsilon_m p_m)$$

$$\text{where } \begin{cases} \varepsilon_k = \pm 1, \varepsilon_m = \pm 1 \text{ and } i = \sqrt{-1} \\ q_k = w_{2k-1} \text{ and } p_k = w_{2k} \end{cases} \quad (\text{B21})$$

Acting on the functions $\sigma_{km\varepsilon_k\varepsilon_m}$ with $\tilde{R}\tilde{\Lambda}$ gives the result:

$$\tilde{R}\tilde{\Lambda} \sigma_{km\varepsilon_k\varepsilon_m} = \exp(-(\alpha_k + \alpha_m) + i2\pi(\varepsilon_k \nu_k + \varepsilon_m \nu_m)) \sigma_{km\varepsilon_k\varepsilon_m}. \quad (\text{B22})$$

Using Equation (B22), we can compute the operator $-\left\{1 - (\tilde{R}\tilde{\Lambda})^{-1}\right\}^{-1}$ on the $\sigma_{km\varepsilon_k\varepsilon_m}$'s:

$$-\left\{1 - (\tilde{R}\tilde{\Lambda})^{-1}\right\}^{-1} \sigma_{km\varepsilon_k\varepsilon_m} = \frac{-1}{1 - \exp((\alpha_k + \alpha_m) - i2\pi(\varepsilon_k\nu_k + \varepsilon_m\nu_m))} \sigma_{km\varepsilon_k\varepsilon_m}. \quad (\text{B23})$$

Away from resonances (i.e., $\varepsilon_k\nu_k + \varepsilon_m\nu_m \cong k$; $k \in \mathbb{Z}$) and for small dampings, only $\sigma_{kk1-1}(\mathbf{w}) = q_k^2 + p_k^2 = \varepsilon_k$ contributes to Equation (B23):

$$\sigma_{\infty;kk1-1} = -\left\{1 - (\tilde{R}\tilde{\Lambda})^{-1}\right\}^{-1} \sigma_{kk1-1} = \frac{-1}{1 - \exp(2\alpha_k)} \sigma_{kk1-1} \approx \frac{1}{2\alpha_k} \sigma_{kk1-1}. \quad (\text{B24})$$

We extract from Equation (C20) the σ_{kk1-1} ($k = 1, 2, 3$) components of $\sigma_{n;\infty}$:

$$\sigma_{\infty;kk1-1}(\mathbf{w}) \approx \left\{ \frac{1}{4\alpha_k} \oint_{s=0}^{s=C} \left\{ \left(B_{2k5}^{-1} \right)^2 + \left(B_{2k-15}^{-1} \right)^2 \right\} \frac{dB_{55}}{ds} ds \right\} \left(q_k^2 + p_k^2 \right). \quad (\text{B25})$$

The mean ‘‘mean emittance’’ is the average of q_k^2 and p_k^2 :

$$\langle \varepsilon_k \rangle = \langle q_k^2 \rangle + \langle p_k^2 \rangle = \frac{1}{2\alpha_k} \oint_{s=0}^{s=C} \left\{ \left(B_{2k5}^{-1} \right)^2 + \left(B_{2k-15}^{-1} \right)^2 \right\} \frac{dB_{55}}{ds} ds. \quad (\text{B26})$$

Hence, we regain the results of Equation (B9) whenever the damping decrement is sufficiently small.

REFERENCES

1. L. Schachinger and R. Talman, *Part. Accel.* **22**, 35 (1987).
2. M.F. Reusch, E. Forest, and J.B. Murphy, in *Proceedings of the 1991 IEEE Particle Accelerator Conference*, IEEE publication 91CH3038-7, p.1651.
3. K. Oide and H. Koiso, *Phys. Rev. E*, **47**, 2010 (1993).
4. E. Forest and K. Ohmi, ‘‘Symplectic integration of complex wigglers,’’ KEK Report 92–14 (1992).
5. E. Forest and K. Hirata, ‘‘A contemporary guide to beam dynamics,’’ KEK Report 92–12 (1992).
6. M. Berz, *Part. Accel.* **24**, 109 (1989). This article describes the original ‘‘DA package’’ of Berz which we use in our tracking codes for automatic differentiation.
7. E. Forest, J. Irwin and M. Berz, *Part. Accel.* **24**, 91 (1989). This describes the essence of the library LIELIB which we use for perturbation theory on the map. We added the ability to analyze non-symplectic maps which is not described in this paper.
8. M. Berz, *Part. Accel.* **24**, 109 (1989).
9. L.M. Healy, University of Maryland Ph.D. thesis. See also Healy, L.M., A.J. Dragt and I.M. Gjaja, *J. Math. Phys.* **33**, 1948 (1992).
10. A.J. Dragt, *Part. Accel.* **12**, 205 (1982).
11. K. Hirata and F. Ruggiero, CERN, LEP Note 611 (1988).

12. A.W. Chao, *J. Appl. Phys.*, **50**, 595 (1979).
13. K. Ohmi, K. Hirata and K. Oide, *Phys. Rev. E*, **49**, 751 (1994).
14. E. Forest and R.D. Ruth, *Physica D* **43**, 105 (1990).
15. H. Yoshida, *Phys. Let. A*, **150**, 262 (1990).
16. M. Suzuki, *Phys. Let. A*, **146**, 319 (1990). For a proof of the “must-drift-backwards” conjecture in integrators of order higher than 2, see *J. Math. Phys.* **32**, 400 (1991).
17. E. Forest, J. Bengtsson and M. Reusch, *Phys. Let. A*, **158**, 99 (1991).
18. K. Hirata, “An introduction to SAD”, in *Proceeding of the 2nd ICFA Beam Dynamics Workshop*, CERN 88-04 (1988). A final reference on this code is still in the making.
19. F.C. Iselin, *Part. Accel.* **17**, 143 (1985).
20. E. Forest and J. Milutinovic, *Nucl. Instrum. Meth.*, **A269**, 474 (1988).
21. M. Sands, *Stanford Linear Accelerator Report SLAC-121*, (1970).
22. E. Forest and J. Milutinovic, *Nucl. Instrum. Meth.*, **A269**, 474 (1988).
23. A. Piwinski, in *Proceeding of the CERN Accelerator School, General Accelerator Physics* (Gif-sur-Yvette, Paris, France), CERN 85-19 (1985).